Pramāṇa – J. Phys., Vol. 25, No. 1, July 1985, pp. 49–61. © Printed in India.

Transport in boundary layer of divertor tokamaks

S B HALDER and P DASGUPTA
Department of Physics, University of Kalyani, Kalyani 741 235, India

MS received 26 November 1984; revised 24 April 1985

Abstract. Study of transport in the boundary layer of tokamak plasma in presence of magnetic divertors is extended to the second order in ion collision frequency. Numerical results for ion and energy losses to the collector plates are presented for toroidal and poloidal divertors. For the toroidal case, the Wiener-Hopf solution for the second order distribution function is obtained. An error occurring in an earlier first order calculation is pointed out and corrected first order fluxes are also given. For the poloidal divertor, asymmetry observed in ion and energy transport is found to persist in the second order result.

Keywords. Tokamak; plasma; divertor; drift kinetic equation.

PACS No. 51·10; 52·55

1. Introduction

Despite some handicaps, the divertor concept remains one of the possible means of impurity control in tokamak plasma which is an important aspect to be looked after if a tokamak is to be used as a reactor. Perhaps even more important is the possibility of using the divertor as the ash and heat exhaust in the reactor system. A divertor usually affects both the MHD stability (Charlton *et al* 1981) and transport of the plasma inside a tokamak in a non-trivial way because it imposes a magnetic field separatrix at the edge of the plasma. The transport is mainly governed by plasma diffusion into the scrape-off layer which in a steady-state reactor should balance the rate at which particles are lost to the divertor. Since this provides the boundary condition to the transport codes (Hinton *et al* 1972) to be used for the plasma interior, a careful study of the boundary layer transport is necessary.

Such studies have been undertaken in the past by Hinton and Hazeltine (1974) and Daybelge (1981) for poloidal divertor and by Daybelge and Bein (1977) for toroidal divertor geometry on the basis of drift kinetic theory. A crucial assumption common to all these works is that ions in the boundary layer are weakly collisional, *i.e.* $\bar{\nu}_{ii}\tau_{\parallel} \ll 1$, $\bar{\nu}_{ii}$ being the average ion-ion collision frequency and $\tau_{\parallel}$ being the time period of parallel motion of the ions around a drift orbit. This assumption has been exploited to linearize the collision operator in the drift kinetic equation using the collisionless solution as the first approximation. The solution of the kinetic equation is then used to calculate the particle and energy losses to the collector plate.

In this paper we pursue the perturbative approach improving the approximation for the collision operator to the next order in collision frequency to obtain corrections to

the first order results. The motivation is derived from two reasons. Firstly, the consistency of the weak collisionality assumption and hence the validity of the perturbation theory, is not obvious. In fact the collisionless solution in the immediate neighbourhood of the separatrix is characterized by such anisotropy as may drive instabilities of the loss cone type leading to enhancement of field fluctuations and therefore to enhancement of the average collision frequency. Secondly, the fluxes in the boundary layer need to be calculated as accurately as possible if these are used to specify the boundary conditions on transport of the interior plasma. Hence it is worthwhile to consider higher order corrections to the particle and energy fluxes in the scrape-off region.

The weak ion collisionality has been justified *a posteriori* by a consistency argument. The weak ion collisionality together with neoclassical transport for the interior plasma can be shown to lead to the result that while the electron temperature profile drops considerably near the separatrix, the ions remain almost uniformly hot all over the section of the torus (Stacey 1974). This in its turn would imply smallness of the ion collision frequency.

Besides this assumption, we shall retain most other simplifying assumptions used in the earlier investigations. The inverse aspect ratio will be treated as small. The banana orbits will not have any role to play in the calculation of fluxes merely because the particles which reach the divertor plates, which we assume to be perfect absorbers, get lost and can no longer remain trapped in banana orbits. Backstreaming of particles along the intercepted orbits is completely neglected. The orbits are also assumed to be free from any influence of the electric field which can be shown in the collisionless approximation to be small near the separatrix as a consequence of quasi-neutrality. Finally we assume a simplified geometry which for toroidal divertors (similar to poloidal limiter plate) is shown in figure 1, and for poloidal divertors is shown in figure 6.

In §2 we present our study of toroidal divertors. For the preliminaries and details of the first order calculation, the reader is referred to the paper of Daybelge and Bein (1977). However, we point out an error occurring in their first order calculation and we give the correct results in the text. The Wiener-Hopf solution for the second order distribution function and numerical results for the second order fluxes are then given.

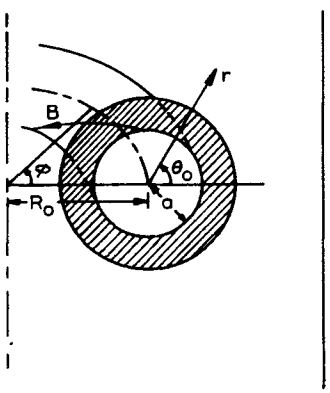

Figure 1. Geometry of the poloidal limiter plate (toroidal divertor).

In §3 we deal with the case of poloidal divertors which are of greater practical significance. The interesting phenomenon of asymmetric transport has been explained in the first order theory of Daybelge (1982). We show that the asymmetry persists and, in fact, is enhanced in the second order.

2. Toroidal divertors

2.1 *The diffusion equation in the scrape-off layer*

The drift kinetic equation for the ion distribution function f in the boundary layer of a toroidal divertor (which for our purpose is essentially the same as the scrape-off layer of a poloidal limiter (Daybelge *et al* 1977) leads to the non-linear equation

$$q(a)(\partial f/\partial\Phi) = (3z^2/32\pi Nvx^5)\,F(D)(\partial^2 f/\partial\xi^2), \tag{1}$$

where $q(a)$ is the safety factor aB_T/R_0B_p (R_0 and a are the major and minor radii of the torus, B_T and B_p are the toroidal and poloidal fields, $x = \cos\theta_p = v_\parallel/v$, θ_p the pitch angle, $z = \cos\theta - \cos\theta_0$, θ being the polar angle which has the value θ_0 at an arbitrarily chosen initial point (r_0, θ_0, Φ_0) on a particle orbit which satisfies the equation $\tau = \tau_0 - z(\theta_0, \Phi)v(1+x^2/2x)\tau = (r-a)R_0eB_p/aMv_{Ti}$, $\theta = \theta_0 + \Phi/q$, v_{Ti} denoting the ion thermal speed. The boundary layer variable ξ stands for τ_0/δ where $\delta^2 = R_0K\bar{\nu}_{ii}/V_{Ti}$ is a small number for a small ion collision frequency $\bar{\nu}_{ii}$. The safety factor is assumed to be a rational number $q = K/N$. The function $F(D)$ is given by

$$F(D) = [x^2(1+x^2)^2g_{11} + (1-x^2)^3g_{22} + 2x(1-x^2)^{3/2}(1+x^2)g_{12}]_D \tag{2}$$

where D denotes the compliment of the loss regions in velocity space and

$$g_{11} = \int_D dv'(1-p^2)v'^2 f/W^3 \tag{3}$$

$$g_{22} = \int_D dv'[v'^2(1-t^2) + v^2 - 2vv'p]f/W^3 \tag{4}$$

$$g_{12} = \int_D dv'[v - pv']v't f/W^3 \tag{5}$$

with $p = e_v \cdot e_{v'}$, $t = e_\theta . e_{v'}$ and $W = |v - v'|$.

In (1), the collision operator has been approximated by the second-order derivatives which dominate over the lower derivatives near the boundary.

Next, we make a perturbation expansion of f with the parameter δ as the order parameter

$$f = f^{(0)} + f^{(1)} + f^{(2)} + \ldots \tag{6}$$

$$F(D) = F^{(0)}(D) + F^{(1)}(D) + \ldots \tag{7}$$

where $f^{(n)} = O(\delta^n)$ etc., $f^{(0)}$ being the solution in the collisionless approximation. Equation (1) will then be solved at each order with the collision operator of the previous order occurring in the right hand side. Thus

$$q(a)\frac{\partial \overline{f}}{\partial\Phi} = \frac{3z^2}{32\pi Nvx^5}F^{(0)}(D)\frac{\partial^2\overline{f}}{\partial\xi^2} \tag{8}$$

$$q(a)\frac{\partial f^{(2)}}{\partial \Phi} = \frac{3z^2}{32\pi N v x^5}\left[F^{(0)}(D)\frac{\partial^2 f^{(2)}}{\partial \xi^2} + F^{(1)}\frac{\partial^2 \bar{f}}{\partial \xi^2}\right] \tag{9}$$

and so on. Equation (8) for the first order distribution function $\bar{f} = f^{(0)} + f^{(1)}$ shows that the effect of collision is mainly diffusion across the boundary layer. The equations in higher order are inhomogeneous diffusion equations.

Since the diffusion coefficient appearing in (8) depends on Φ, it is convenient to transform the variable Φ to another variable ζ such that (8) takes the form

$$\frac{\partial \bar{f}}{\partial \zeta} = \lambda^{(0)}\frac{\partial^2 \bar{f}}{\partial \xi^2} \tag{10}$$

with $\lambda^{(0)}$ independent of ζ. This is achieved with

$$\zeta = \frac{1}{\gamma}\int d\Phi z^2(\Phi) F^{(0)}(D) \tag{11}$$

$$\gamma = \int_0^{2\pi k} d\Phi z^2(\Phi) F^{(0)}(D) \tag{12}$$

The quantity γ has been so defined as to ensure a normalization $\zeta(\Phi = 0) = 0$ and $\zeta(\Phi = 2\pi K) = 1$. Then (10) is obtained if we set

$$\lambda^{(0)} = \frac{3\gamma}{32\pi N v x^5} \tag{13}$$

The second order equation (9) then can be written in the form

$$\frac{\partial f^{(2)}}{\partial \zeta} = \lambda^{(0)}\frac{\partial^2 f^{(2)}}{\partial \xi^2} + \alpha(\zeta, \xi)\frac{\partial^2 \bar{f}}{\partial \xi^2} \tag{14}$$

where

$$\alpha(\zeta, \xi) = \frac{3}{32\pi N v x^5}\frac{1}{q}\int_0^{2\pi K} d\Phi z^2(\Phi) F^{(1)}(D)$$

The ζ-dependence of $\alpha(\zeta, \xi)$ is entirely due to $F^{(1)}(D)$ which is evaluated putting $\bar{f}(\zeta, \xi)$ in place of f in (3)–(5). Writing $\beta(\zeta, \xi) = \alpha \partial^2 \bar{f}/\partial \xi^2$ we get

$$\frac{\partial f^{(2)}}{\partial \zeta} = \beta + \lambda^{(0)}\frac{\partial^2 f^{(2)}}{\partial \xi^2} \tag{15}$$

2.2 *The first order solution and fluxes*

The analytical solution to equations of the form (8) can be obtained by the Wiener-Hopf technique (Baldwin *et al* 1972). The ion and ion energy flux to the divertor plate can be calculated from the asymptotic behaviour of the solution at $\zeta = 1$ (Hinton and Hazeltine 1974). These have been calculated for the poloidal limiter (equivalently, toroidal divertor) case by Daybelge and Bein (1977). The latter calculation, however, suffers from an error.

The quantity γ defined in (12) receives contributions from the three regions D_1, D_2 and D_3 shown in figure 2. While D_1 and D_2 are independent of Φ, D_3 is not; a fact which makes the computation very laborious. To reduce this labour, Daybelge and Bein (1977) defined a mean $F^{(0)}(D_3)$ which they calculated using an expansion of the

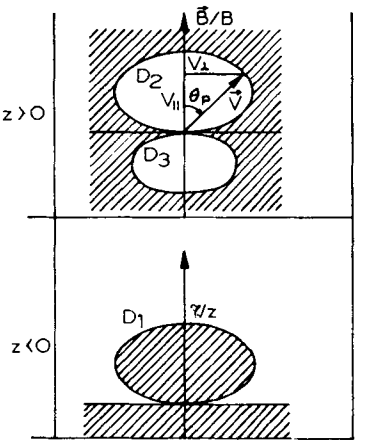

Figure 2. Loss regions (shaded) in the velocity space of counter-moving collision partners for a test particle with $v_\parallel > 0$.

quantity Z defined by $dZ/d\theta = z^2$ which converges very poorly for $|\cos\theta|$ approaching 1 and this has nothing to do with the end points of integration for $F^{(0)}(D)$ where the integrand might vanish. As a matter of fact, the coefficients of the first two terms in that expansion must vanish in an exact calculation. Consequently, figure 8 of their paper is misleading.

We have carried out a fresh computation of these fluxes in the first order for various tokamak parameters calculating everytime the original integral for $F^{(0)}(D_3)$. The results are shown in figures 3 and 4. It is seen that the qualitative feature of the results presented by Daybelge and Bein survive in our first order calculation. The load on the divertor decreases as θ_0 increases to $\pi/2$. However, as we shall show below, the second order correction tends to wash out this effect.

2.3 *Analytic solution of the second order equation*

The second order equation (15) can be transformed, using appropriate boundary conditions, into

$$f^{(2)}(1,\xi) = H(1,\xi) + \frac{1}{\sqrt{2\pi}} \int_{-\infty}^{\infty} d\xi' K(\xi - \xi') f^{(2)}(1,\xi') \tag{16}$$

where

$$H(\zeta,\xi) = \frac{1}{\sqrt{2\pi}} \int_{-\infty}^{\infty} dk \left[A_k(\zeta) - A_k(0)\right] \exp\left[-ik\xi - \lambda^{(0)}k^2\zeta\right] \tag{17}$$

$$A_k(\zeta) = \int d\zeta \beta_k \exp\left(\lambda^{(0)}k^2\zeta\right) \tag{18}$$

$$K(\xi - \xi') = \frac{1}{(2\lambda^{(0)})^{1/2}} \exp\left[-(\xi - \xi')/4\lambda^{(0)}\right] \tag{19}$$

where β_k denotes the Fourier transform of $\beta(\xi)$.

Equation (16) is an inhomogeneous Wiener-Hopf equation which can be solved by

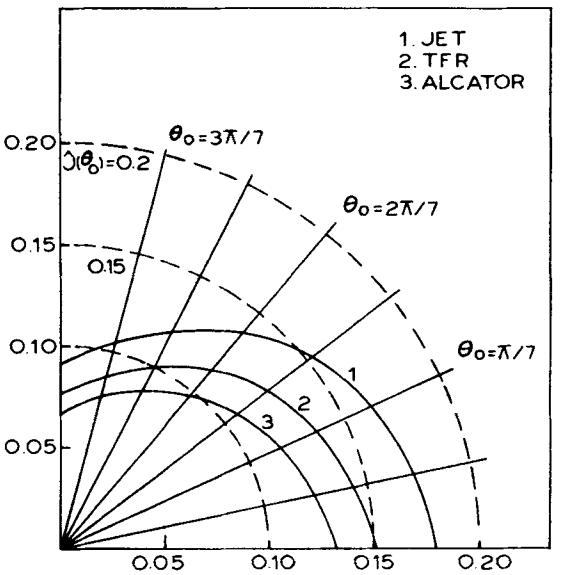

Figure 3. Polar plot for the first order radial ion flux $\hat{J}(\theta_0)$.

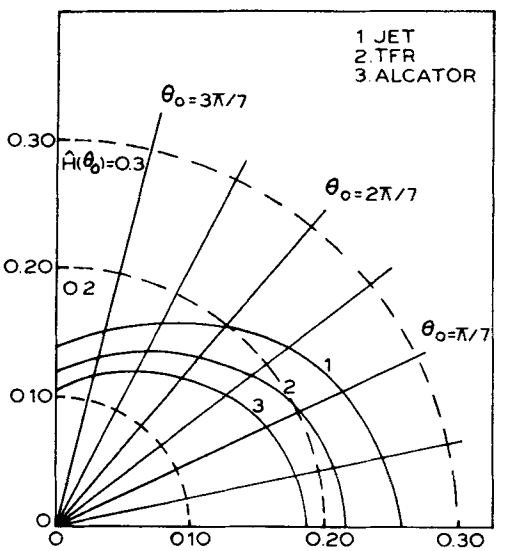

Figure 4. Polar plot for the first order radial ion energy flux $\hat{H}(\theta_0)$.

the standard technique. Denoting by $\tilde{H}(k)$ the Fourier transform of $H(1, \xi)$, we define

$$\Psi_{\pm}(k) = \exp\left[-\frac{k}{2\pi i}\int_{-\infty+i\varepsilon_{\pm}}^{\infty+i\varepsilon_{\pm}} d\eta\, q(\eta)/(\eta-k)\right] \tag{20}$$

$$q(k) = k^{-1}\ln(1-\exp(-k^2)) \tag{21}$$

$$D_{\pm}(k) = \mp\frac{1}{2\pi i}\int_{-\infty+i\varepsilon_{\pm}}^{\infty+i\varepsilon_{\pm}} d\eta\,\tilde{H}(\eta)\Psi_{+}(\eta)/(\eta-k) \tag{22}$$

with $\varepsilon_+ = -\sqrt{\pi}$ and $\varepsilon_- = 0^-$.

Application of the Wiener-Hopf technique then leads to the solution

$$f_\pm(1,\xi) = \frac{1}{\sqrt{2\pi}} \int_\Gamma \mathrm{d}k \left[\frac{\pm Q \mp D_\pm}{\Psi_\pm} \right] \exp(ik\xi) \tag{23}$$

where Γ is a contour running parallel to the real k axis with $0 > \mathrm{Im}\, k > -\sqrt{\pi}$ on it. Analysis of the asymptotic behaviour of $\Psi_\pm$ and $\tilde{H}$ for $|k| \to \infty$ shows that Q in (23) must be a constant with respect to k. This constant can be determined by matching (23) with the bulk solution for $\xi \to -\infty$.

The second order transport coefficients involve the quantity

$$I^{(2)} = \frac{1}{(\lambda^{(0)})^{1/2}} \int_0^\infty \mathrm{d}\xi f^{(2)}(\zeta_0, \xi) \tag{24}$$

which from (23) becomes

$$I^{(2)} = -(2\pi/\lambda^{(0)})^{1/2} \frac{D_+(0) - Q}{\Psi_+(0)} \tag{25}$$

$D_+(0)$ and $\Psi_+(0)$ denote the values at $k = 0$.

2.4 *Second order correction to fluxes*

The second order corrections to the particle and energy fluxes to the limiter plate are given by

$$\bar{J}^{(2)}(\theta_0) = \frac{2\pi a M v_{Ti}^{9/2} \bar{\nu}_{ii}^{1/2}}{R_0^{1/2} e B_p} \int_0^1 x\mathrm{d}x \int_0^\infty \mathrm{d}v\, v^3 \int_0^\infty \mathrm{d}\xi f^{(2)+} \tag{26}$$

$$\bar{H}^{(2)}(\theta_0) = \frac{\pi a M^2 v_{Ti}^{13/2} \bar{\nu}_{ii}^{1/2}}{R_0^{1/2} e B_p} \int_0^1 x\,\mathrm{d}x \int_0^\infty \mathrm{d}v\, v^5 \int_0^\infty \mathrm{d}\xi f^{(2)+} \tag{27}$$

In principle, the second order solution (23) can be put in these expressions to obtain the values of $\bar{J}^{(2)}$ and $\bar{H}^{(2)}$ for various θ_0. However, since (23) involves contour integrals in the complex k-plane together with the various Fourier transformed quantities, it does not provide a convenient expression for numerical computation. We have therefore, worked directly with the inhomogeneous equation (16) and solved it numerically by iteration. The convergence of the iterative procedure turns out to be fairly rapid, stabilizing usually after 4 or 5 iterations. The solution is then used for computation of $\bar{J}(\theta_0)$ and $\bar{H}(\theta_0)$. The results are shown in figure 5.

It is seen that the second order correction is small and positive. The smallness assures us of the validity and consistency of the perturbative approach. As emphasized in §1, the second order correction may still be considered important when the results of the above theory are used as boundary conditions for tokamak transport codes and also because the resulting loss cone instabilities may tend to increase the collision frequency $\bar{\nu}_{ii}$.

Finally, we note that the second order correction is proportionately larger near $\theta_0 \sim \pi/2$ thus tending to compensate the angular variation of the load on the limiter plate indicated by the first order calculation.

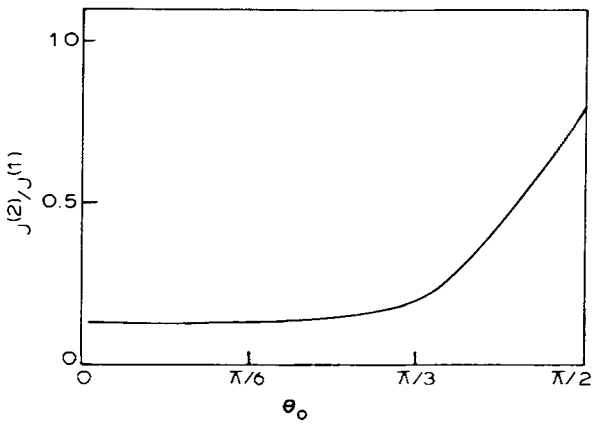

Figure 5. Second order correction to the radial ion flux for JET.

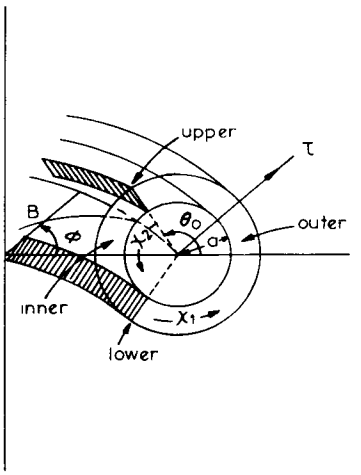

Figure 6. Geometry of the poloidal divertor with the collector plates positioned at $\pm\theta_0$. The field lines are directed away from the viewer.

3. Poloidal divertors

3.1 *Asymmetric transport*

The poloidal divertor is a widely tried device for impurity control and other purposes in tokamaks. Experiments on a few tokamaks including PDX, Ti2 and ASDEX have revealed asymmetries in the transport properties of the divertor scrape-off layer. Qualitative explanation of these asymmetries which elude the oversimplified one-dimensional codes was given by Daybelge (1981) on the basis of drift kinetic theory in the first order. Since these asymmetries lead to preferential loading of the divertor plates, their quantitative study is important for the design of any machine using poloidal divertors. We calculate here the relevant fluxes to the second order in ion collision frequency.

The asymmetries observed with double-null poloidal divertors (figure 6) are of two

kinds. There is an asymmetry between the fluxes on the upper and the lower collector plates. Secondly, there is an asymmetry between the fluxes on the inner faces and the outer faces of both the plates. The latter is stronger than the former and is comparatively easy to understand. It arises out of the difference in the arc lengths from plate to plate along the inner and outer regions. The upper-lower asymmetry is more controversial and, being a weaker effect, demands greater accuracy both in experimental measurement and in theoretical calculation. Since the system is otherwise symmetric, a possible origin of this asymmetry lies in the direction of the toroidal field causing shift in the drift orbits. It is this particular feature of the asymmetric transport in the boundary layer that we calculate more accurately in the following. We shall show that the second order calculation leads to a clear enhancement of the upper-lower asymmetry.

3.2 *The second order equation*

The diffusion equation for the scrape-off layer of a poloidal divertor leads in the second order in δ to the equation (for $x > 0$)

$$\frac{\partial f^{(2)+}}{\partial \chi_1} = h_1^+ + \lambda_1 \frac{\partial^2 f^{(2)+}}{\partial \chi_1^2}, \quad 0 < \chi_1 < 1 \tag{28}$$

$$\frac{\partial f^{(2)+}}{\partial \chi_2} = h_2^+ + \lambda_2 \frac{\partial^2 f^{(2)+}}{\partial \chi_2^2}, \quad 0 < \chi_2 < 1 \tag{29}$$

where χ_1, χ_2, λ_1 and λ_2 are the same as defined in Daybelge's (1981) paper and

$$h_{1,2}^+ = \lambda_{1,2}^{(1)} \frac{\partial^2 \overline{f}^+}{\partial \xi^2} \tag{30}$$

with $\lambda_{1,2}^{(1)}$ denoting first order corrections to λ_1 and λ_2. Formal solution of the initial value problem corresponding to (28) and (29) leads to

$$f^{(2)+}(\xi, \chi_i) = H_i^+(\xi, \chi_i) + \frac{1}{2\pi} \int_{-\infty}^{\infty} \mathrm{d}k \int_{-\infty}^{0} \mathrm{d}\xi' f^{(2)+}(\xi', 0) \exp[ik(\xi - \xi') - \lambda_i k^2 \chi_i] \tag{31}$$

with

$$H_i^+(\xi, \chi_i) = \int_{-\infty}^{\infty} \mathrm{d}\xi' \int_0^{\chi_i} \mathrm{d}\chi_i' h_i(\xi', \chi_i') \exp[-(\xi - \xi')^2 / 4\lambda_i(\chi_i - \chi_i')] \tag{32}$$

Further use of boundary conditions yields the inhomogeneous integral equation

$$\begin{aligned} f^{(2)+}(\xi, \chi_1 = 1) = H_1^+(\xi, \chi_1 = 1) &+ \frac{1}{(4\pi\lambda_1)^{1/2}} \\ &\times \int_{-\infty}^{\infty} \mathrm{d}\xi' H_2^+(\xi', \chi_2 = 1) \exp[-(\xi - \xi')^2 / 4\lambda_1] \\ &+ \frac{1}{(4\pi\lambda)^{1/2}} \int_{-\infty}^{0} \mathrm{d}\xi' f^{(2)+}(\xi', \chi_1 = 1) \\ &\times \left\{1 - \operatorname{erf}\left[\frac{r\xi + \xi'/r}{\sqrt{\lambda}}\right]\right\} \exp[-(\xi - \xi')^2 / 4\lambda] \end{aligned} \tag{33}$$

and a similar equation for $f^{(2)+}(\xi, \chi_2 = 1)$. In (33) we have put $r = (\lambda_2/\lambda_1)^{1/2}$ and $\lambda = \lambda_1 + \lambda_2$.

By interchanging the loss regions corresponding to $x > 0$ and $x < 0$, the equation for particles with $x < 0$ can similarly be derived. The resulting equation for $f^{(2)-}$ has a structure similar to (33) though the λ's become different. These equations are, in general, not of the Wiener-Hopf type and must be solved numerically.

3.3 *The second order fluxes and asymmetries*

The upper-outer fluxes are calculated from $f^+(\chi_1 = 1)$, the upper-inner from $f^-(\chi_1 = 1)$, the lower outer from $f^+(\chi_2 = 1)$ and the lower-inner from $f^-(\chi_2 = 1)$. The inner-outer asymmetry evidently persists in the second order as our equations predict entirely different solutions for $f^{(2)+}$ and $f^{(2)-}$. The asymmetry disappears at $\theta_0 = \pm\pi/2$ as expected from the symmetry of the situation. The upper-lower symmetry is inescapable even at that plate position because λ_1 and λ_2 are still unequal.

We have carried out numerical calculation for the second order fluxes for $\theta_0 = \pm\pi/2$. Equation (33) and its counterpart for $\chi_2 = 1$ have been solved by straightforward iteration which is found to converge fairly rapidly (figure 7). Typical behaviour of the solution for different x and v is illustrated in figures 8 and 9. The second order corrections to the fluxes are displayed in figures 10 and 11. The mean percentage correction in the second order to the energy-flux asymmetry seems to be slightly higher than that to the ion-flux asymmetry between the upper and the lower collector plates. In figures 12 and 13 we show the radial variation of the upper-lower asymmetry parameters

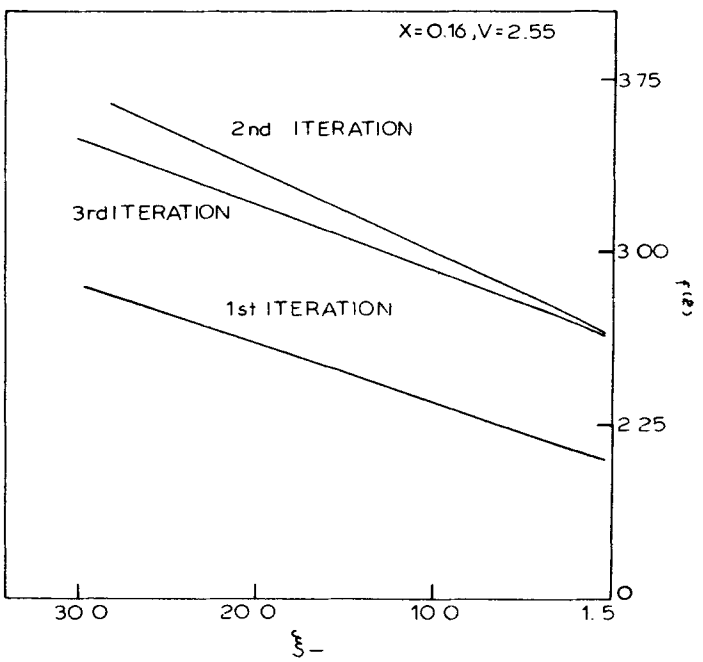

Figure 7. Typical result of the first three iterations of the second order equation for the distribution function.

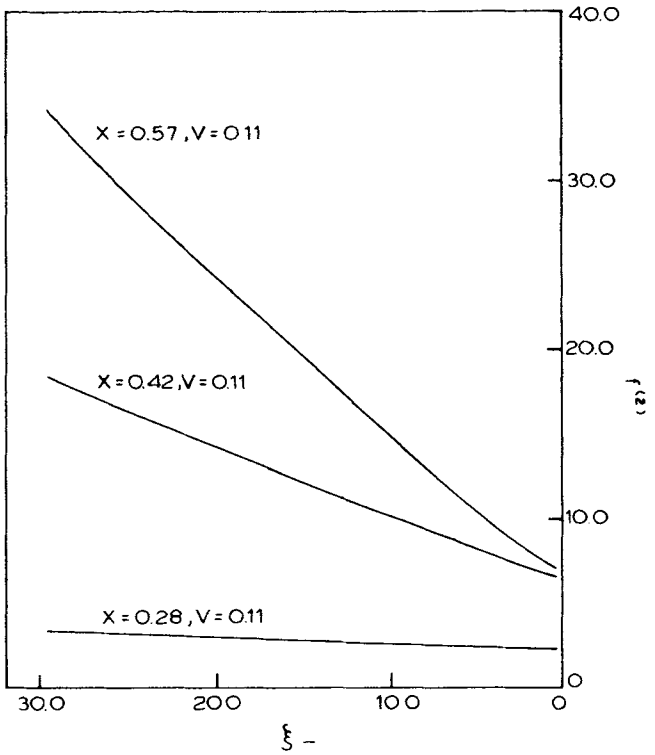

Figure 8. Variation of the second order distribution function with x.

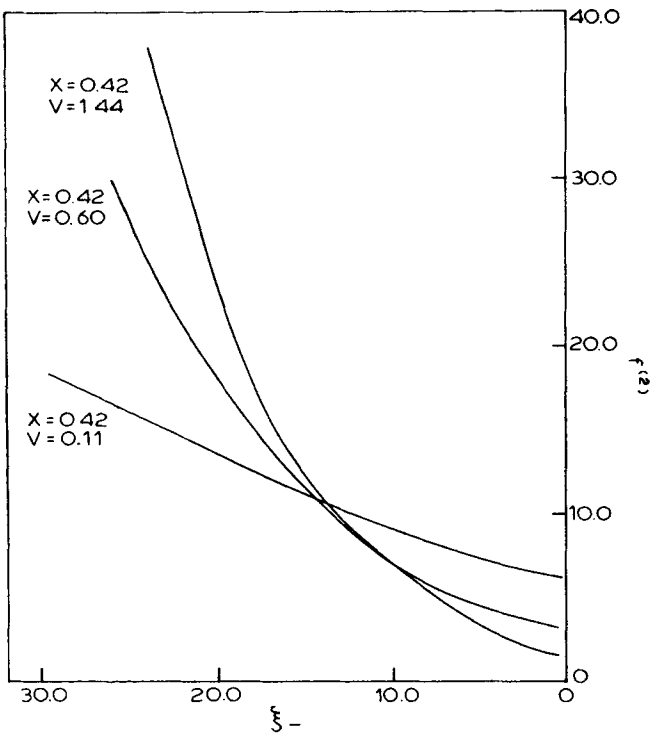

Figure 9. Variation of the second order distribution function with v.

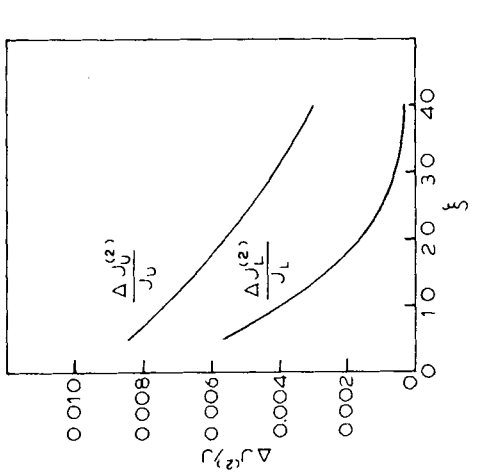

Figure 10. Second order correction for the ion flux to the upper and lower collector plates at $\theta_0 = \pm 90°$.

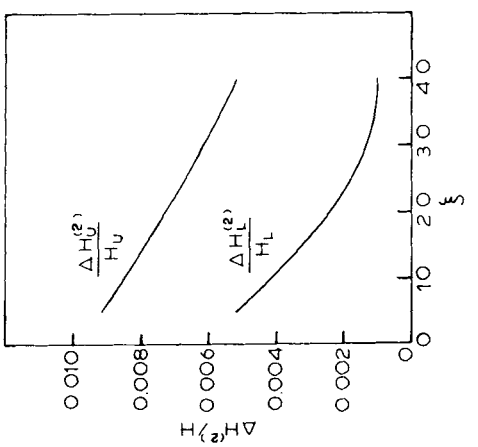

Figure 11. Second order correction for the ion energy flux to the upper lower plates at $\theta_0 = \pm 90°$.

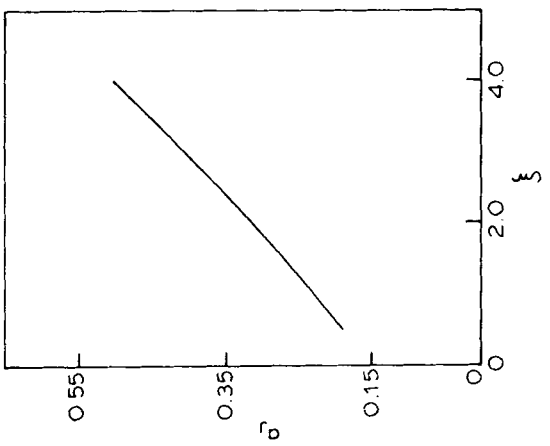

Figure 12. Radial distribution of the upper lower asymmetry a_J in the ion flux calculated to the second order.

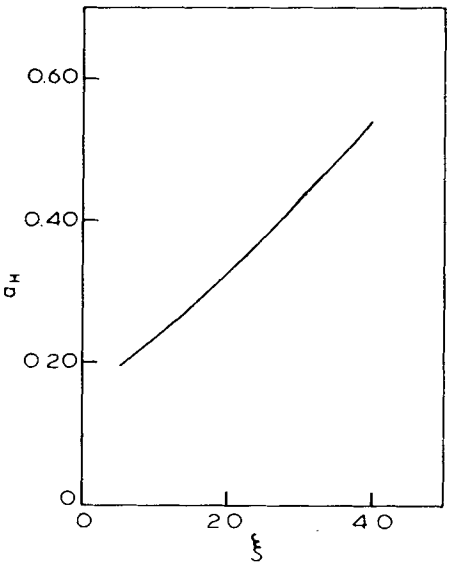

Figure 13. Radial distribution of the upper lower asymmetry a_H in the ion energy flux calculated to the second order.

$a_J = (J_U - J_L)/(J_U + J_L)$ for the total ion flux and $a_H = (H_U - H_L)/(H_U + H_L)$ for the total energy flux. The asymmetry steadily increases toward the outer region of the collector plates.

References

Baldwin D E, Cordey J G and Watson C H 1972 *Nucl. Fusion* **12** 307
Charlton L A, Dory R A, Strickler D J and Lee D K 1981 *Nucl. Fusion* **21** 1334
Daybelge U 1981 *Nucl. Fusion* **21** 1589
Daybelge U and Bein B 1977 *Phys. Fluids* **20** 1777
Hinton F L and Hazeltine R D 1974 *Phys. Fluids* **17** 2236
Hinton F L, Wiley J C, Duchs D F, Furth H P and Rutherford P H 1972 *Phys. Rev. Lett.* **29** 698
Stacey W M Jr 1974 *Nucl. Fusion* **14** 219